

A Role for Piwi and piRNAs in Germ Cell Maintenance and Transposon Silencing in Zebrafish

Saskia Houwing,^{1,7} Leonie M. Kamminga,^{1,7} Eugene Berezikov,¹ Daniela Cronembold,² Angélique Girard,³ Hans van den Elst,⁴ Dmitri V. Filippov,⁴ Heiko Blaser,⁵ Erez Raz,⁵ Cecilia B. Moens,⁶ Ronald H.A. Plasterk,¹ Gregory J. Hannon,³ Bruce W. Draper,² and René F. Ketting^{1,*}

¹Hubrecht Laboratory, Uppsalalaan 8, 3584 CT, Utrecht, Netherlands

²Molecular and Cellular Biology, University of California, Davis, One Shields Avenue, Davis, CA 95616, USA

³Cold Spring Harbor Laboratories, 1 Bungtown Road, New York, NY 11724, USA

⁴Leiden Institute of Chemistry, Leiden University, P.O. Box 9502, 2300 RA, Leiden, Netherlands

⁵Germ Cell Development, Max Planck Institute for Biophysical Chemistry, Göttingen 37077, and Institute of Cell Biology, ZMBE, University of Münster, Münster 48149, Germany

⁶Division of Basic Science, Fred Hutchinson Cancer Research Center, HHMI, B2-152, 1100 Fairview Avenue North, Seattle, WA 98019, USA

⁷These authors contributed equally to this work.

*Correspondence: ketting@niob.knaw.nl

DOI 10.1016/j.cell.2007.03.026

SUMMARY

Piwi proteins specify an animal-specific subclass of the Argonaute family that, in vertebrates, is specifically expressed in germ cells. We demonstrate that zebrafish Piwi (Ziwi) is expressed in both the male and the female gonad and is a component of a germline-specifying structure called nuage. Loss of Ziwi function results in a progressive loss of germ cells due to apoptosis during larval development. In animals that have reduced Ziwi function, germ cells are maintained but display abnormal levels of apoptosis in adults. In mammals, Piwi proteins associate with approximately 29-nucleotide-long, testis-specific RNA molecules called piRNAs. Here we show that zebrafish piRNAs are present in both ovary and testis. Many of these are derived from transposons, implicating a role for piRNAs in the silencing of repetitive elements in vertebrates. Furthermore, we show that piRNAs are Dicer independent and that their 3' end likely carries a 2'O-Methyl modification.

INTRODUCTION

Argonaute proteins represent a large protein family of which members are found in archaeobacteria and eukaryotes (Carmell et al., 2002). These proteins are at the core of an RNA-silencing machinery that uses small RNA molecules as guides to identify homologous sequences in RNA or DNA. The effects that are induced by Argonaute

proteins include the induction of histone and DNA methylation, deletion of DNA sequences, mRNA breakdown, and inhibition of translation; the specificity of these processes is in part determined by the identity of the Argonaute protein involved (Zamore and Haley, 2005). Argonaute proteins are characterized by the presence of two protein domains: the PAZ domain and the Piwi domain. The PAZ domain is an RNA-binding motif that has been shown to bind the 3' end of short RNAs, and the Piwi domain is structurally similar to the RNaseH catalytic domain (Lingel and Sattler, 2005; Parker and Barford, 2006). Some Argonaute proteins have been shown to possess endonucleolytic activity (Liu et al., 2004), cleaving the target mRNA opposite the phosphodiester bond between bases 10 and 11 of the small RNA (Elbashir et al., 2001).

In animals, the Argonaute protein family can be subdivided into two distinct classes (Figure S1). The most well-studied class is the Ago family. Ago proteins have been shown to function together with short interfering RNAs (siRNAs) and micro RNAs (miRNAs; Carmell et al., 2002). These small RNAs are derived from inter- or intramolecular double-stranded RNA (dsRNA) molecules, respectively, through processing by an RNaseIII enzyme named Dicer (Bernstein et al., 2001). Then, one of the two strands of the approximately 21 nucleotide product is loaded into an Argonaute protein. In mammals siRNAs associate primarily with Ago2, while miRNAs are found in association with all four Ago family members (Liu et al., 2004; Meister et al., 2004). The thermodynamic properties of the double-stranded intermediate influence which strand will complex with the Argonaute protein (Khvorova et al., 2003; Schwarz et al., 2003). In extreme cases, as with most miRNAs, only one of the two strands is incorporated. In contrast, usually both strands of an siRNA duplex can be found in Argonaute complexes,

though the relative abundance of each may differ. The Argonaute-small-RNA complex (RISC, RNA-Induced Silencing Complex) then uses the small RNA to identify and silence homologous targets.

The second branch of the Argonaute proteins in animals represents the much more poorly understood Piwi proteins, which are named after the founding member of this class: *Drosophila* Piwi (Cox et al., 1998). These proteins also contain both a PAZ and a Piwi domain, and some have been shown to be involved in RNAi-like processes in *Drosophila* (Pal-Bhadra et al., 2002). In most animals studied so far, Piwi proteins are expressed specifically in the germline (Cox et al., 2000; Kuramochi-Miyagawa et al., 2001). In contrast to the Ago-family members, the Piwi proteins do not (or do, but to a lesser extent) associate with siRNAs and/or miRNAs. Only recently did it become clear that the Piwi proteins in mammals associate with a separate class of germ-cell-specific small RNA molecules named Piwi-Interacting RNAs (piRNAs; Aravin et al., 2006; Girard et al., 2006; Grivna et al., 2006a; Lau et al., 2006). However, the function of these piRNAs has not been determined.

It is unclear so far whether the function of Piwi in germline development is evolutionarily conserved from invertebrates to vertebrates. In *Drosophila*, Piwi has been shown to be required for the maintenance and behavior of germline stem cells through both cell-autonomous and cell-nonautonomous mechanisms (Cox et al., 1998, 2000). In addition, Piwi and a second family member, Aubergine (Aub), have been shown to play a role in RNAi (Kennerdell et al., 2002; Pal-Bhadra et al., 2002). Similarly, the two *piwi*-related genes in *C. elegans*, *prg-1* and *prg-2*, are also required for the maintenance of mitotic germline stem cells (Cox et al., 1998). By contrast, Piwi expression in mammals appears to be limited to the male germline, and mutations in the mouse *piwi* genes *miwi* and *mili* affect meiotic progression of developing sperm but do not affect the maintenance of mitotic germ cells (Deng and Lin, 2002; Kuramochi-Miyagawa et al., 2004). Here we present a study on *ziwi* and associated piRNAs, implicating roles in germ cell maintenance and transposon silencing in the germline of the zebrafish. Our data also suggest a Dicer-independent pathway for piRNA production.

RESULTS

The Zebrafish Genome Encodes Two Piwi Homologs

In the zebrafish genome (Ensembl version 41) two clear Piwi homologs can be identified among all the known or predicted proteins: ENSDARG00000041699 (*ziwi*) and ENSDARG00000062601 (*zili*, or *piwil2*). Sequence comparison with *piwi* members from other species reveals that *Ziwi* most likely is the ortholog of the mammalian MIWI and HIWI proteins (Figure S1A), while *Zili* clusters with HILI and MILI. In this study we focus on *ziwi*. Using in situ hybridizations we find that *ziwi* expression is gonad specific as previously shown (Tan et al., 2002) and is expressed only in germ cells (Figures 1 and S1B). These

results are further supported by RT-PCR on RNA from wild-type and agametic testis (Weidinger et al., 2003; Figure S1C).

Ziwi Localizes to Nuage in Early Embryos and Germ Cells

Using an affinity-purified version of the *Ziwi* antibody that recognizes a gonad-specific protein of approximately 95 kDa (Figure 1A), we performed immunohistochemistry. We find that maternally provided *Ziwi* protein localizes to granules that cluster along the cleavage planes in two and four cell embryos, which is strikingly similar to the characteristic localization of *vasa* mRNA at these stages (Figure 1B; Yoon et al., 1997). This structure has been described before as nuage, and cytoplasm containing this structure has been shown to be necessary for primordial germ cell (PGC) specification in zebrafish (Hashimoto et al., 2004).

After 24 hr of development we detect *Ziwi* only in PGCs. In these cells *Ziwi* localizes to large perinuclear aggregates, similar to what has been previously described for the *Vasa* and *Dead-end* proteins (Weidinger et al., 2003). To test whether these perinuclear *Ziwi* granules correspond to those previously described granules, we injected mRNA encoding a myc-tagged version of *Vasa* and assayed for colocalization. Indeed, we find perfect colocalization of *Ziwi* and Myc-*Vasa* in these granules (Figure 1C).

In the adult, *Ziwi* is found in both female (Figures 1D and 1E) and male germ cells (Figure 1F), where expression appears strongest in the mitotic and early meiotic stages of germ cell differentiation. In later stages of oogenesis we find *Ziwi* to be localized in granules along the cortex, a region where *vasa* mRNA is also located (Braat et al., 1999). Lastly, we find that *Ziwi* is a predominantly cytoplasmic protein, as judged from the steady-state levels revealed by immunohistochemistry.

Loss of Ziwi Triggers Germ Cell Apoptosis

To study the role of the *Ziwi* in development and function of the zebrafish germline, we screened for mutant alleles in ENU-mutagenized libraries (Draper et al., 2004; Wienholds et al., 2003). We identified three premature stop alleles and two missense mutations that are predicted to be deleterious (Figure 2A). In all allelic combinations examined so far, we have found that *ziwi* homozygous mutants are viable. As adults, however, 100% of the animals homozygous for the premature stop alleles are phenotypically male (see Supplemental Data) and are agametic, indicating that *Ziwi* function is required for germ cell development (Figure 2B).

We first determined at what developmental stage germ cells were lost in *ziwi* mutants. Using *vasa* as a marker (Yoon et al., 1997), we found that wild-type and mutant gonads had similar germ cell numbers at two weeks of age, indicating that zygotic expression of *ziwi* was not required for the specification or early maintenance of germ cells (Figures S2A and S2B). In contrast, in 3-week-old gonads, germ cells were greatly reduced or absent in *ziwi* mutants,

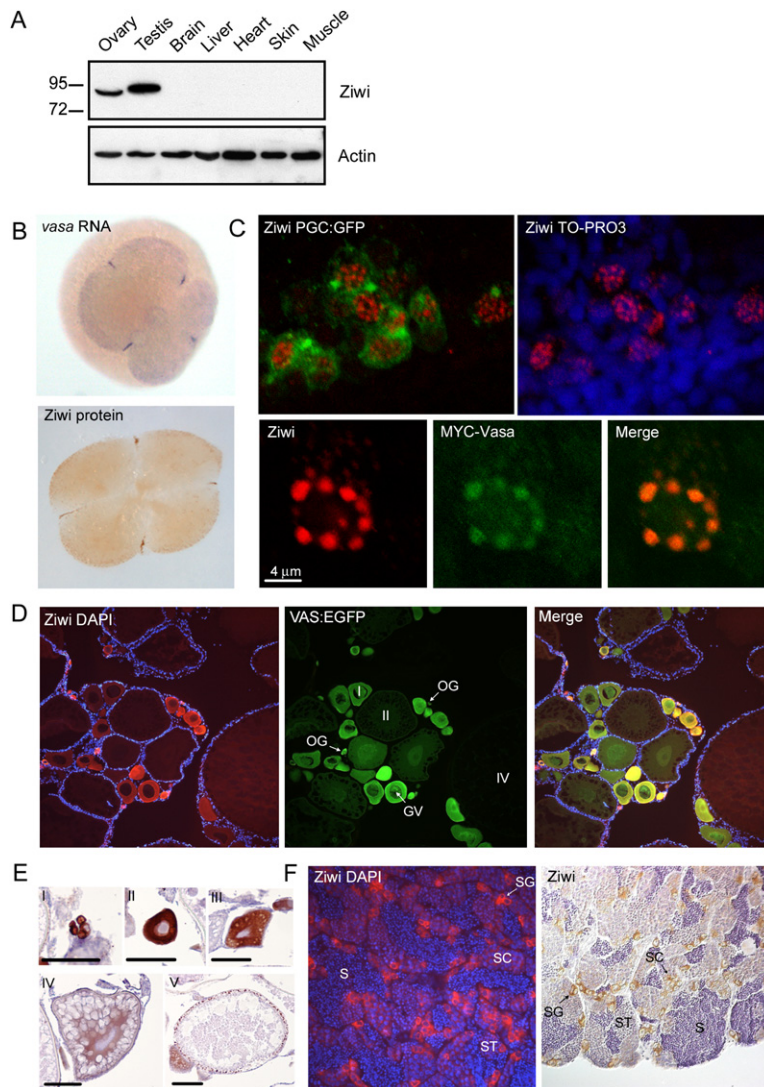


Figure 1. Zivi Subcellular Localization

(A) Western blot shows specific expression of Zivi in testis and ovary.

(B) Zivi protein is maternally provided and localizes to granules at the cleavage planes in four cell embryos similar to *vasa* mRNA.

(C) At 24 hpf Zivi (red) localizes to distinct perinuclear granules in the PGCs (upper two panels). These granules also contain Vasa (lower three panels).

(D) Zivi (red) in ovary is expressed in oogonia and stage I oocytes. Vasa (in green) is expressed in all stages of oogenesis. Stages of oogenesis are oogonia (OG), stage I oocytes (7–140 μm ; I), stage II oocytes (140–340 μm ; II), stage III oocytes (340–690 μm ; not in picture; III), and stage IV oocytes (0.69–0.73 mm; IV), and stage V oocytes (0.69–0.73 mm; V) (Selman et al., 1993).

(E) Zivi expression in various stages of oocytes is visualized by DAB staining to reveal lower levels of expression in later stage oocytes. I indicates oogonia; II indicates Stage I; III indicates Stage II; IV indicates Stage III; and V indicates Early stage V. Scale bar is 100 μm .

(F) Zivi (left panel, red, or right panel, brown) in testis is expressed in spermatogonia and spermatocytes. Stages of spermatogenesis are spermatogonia (SG), spermatocytes (SC), spermatids (ST), and sperm (S).

while they were readily detectable in wild-type (Figure 2D). At 40 days of development no germ cells can be detected in *zivi* mutants (Figure S2F; Table S1). Because *vasa* is expressed not only in PGCs but also in differentiating germ cells, these data argue that *zivi* mutant germ cells do not enter a germ cell differentiation pathway.

We next asked if germ cells in *zivi* mutant gonads were disappearing as a result of apoptosis. We assayed for the presence of apoptotic cells at 3 weeks of development in both wild-type and mutant gonads by scoring for the presence of Caspase-3 immunoreactivity. We observe apoptosis in mutant gonads but not in those isolated from wild-type fish (Figure 2E). This result suggests that loss of germ cells in *zivi* mutants is a consequence of apoptosis. We cannot at this time, however, rule out the possibility that some *zivi* mutant germ cells take on a somatic cell fate.

We also examined animals that had reduced levels of Zivi function. We found that animals carrying one mis-

sense allele (N686K) and one premature stop allele (Q543STOP) have germ cells as adults but display varying degrees of fertility (not shown). To determine the cause of subfertility, we asked if *zivi*(Q543STOP/N686K) individuals had an increase in apoptosis compared to wild-type as evidenced by Caspase-3 immunostaining. Indeed, we find elevated levels of apoptosis (Figure 2C). We cannot assign all the apoptosis events to one particular stage of sperm development; rather we find that various stages of differentiating sperm cells enter apoptosis. As a result of the ongoing apoptosis of the germ cells, the transheterozygous fish show a clear reduction in the number of mature sperm in the tubules (Figure 2C). We also observe a small but consistent increase in apoptosis in *zivi*(Q543STOP/+) animals. Together, these results argue that the role of *zivi* in preventing germ cell apoptosis is dose dependent, although we cannot say whether this role is direct or indirect.

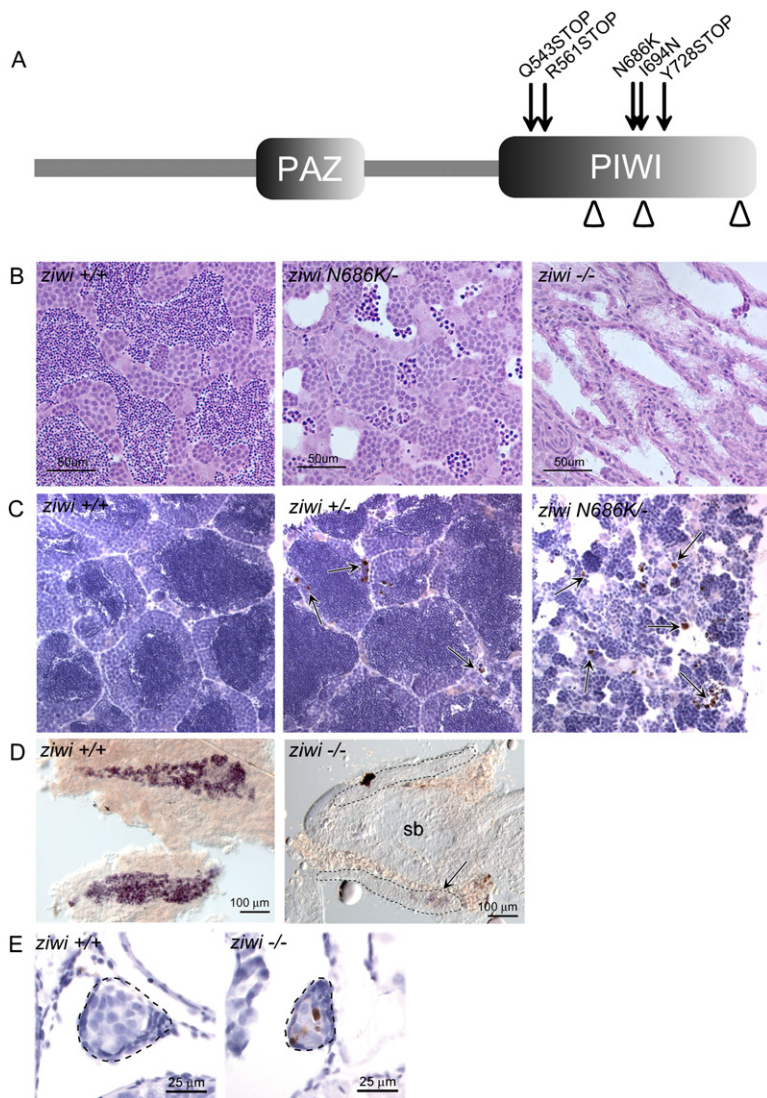


Figure 2. Zivi Is Necessary for the Maintenance of the Germline

(A) Overview of Zivi with PAZ and PIWI domain is shown. DDH motif is indicated by arrowheads. Three STOP mutations—Q543STOP (hu2479), R561STOP (fh219), and Y728STOP (fh221)—and two missense mutations—N686K (hu2410) and I694N (fh222)—are located in the PIWI domain of zivi.

(B) Hematoxylin and eosin staining of wild-type (left), *zivi(Q543STOP/N686K)* (middle), and *zivi -/-* (right) testis is shown. *Zivi(Q543STOP/N686K)* testis show fewer germ cells with almost no sperm. *Zivi(Q543STOP)* mutants have germ cell-depleted testis. (C) Caspase-3 staining (brown) shows apoptotic cells, indicated by arrows. In wild-type testis very few apoptotic cells are observed. Heterozygous *zivi(Q543STOP/+)* testis show several apoptotic cells, but overall morphology is wild-type. *Zivi(Q543STOP/N686K)* transheterozygous mutants have few, if any, sperm cells, and many germ cells are apoptotic.

(D) Whole mount in situ hybridization of wild-type and *zivi(R561STOP/Y728STOP)* gonads at 20 dpf, with staining for *vasa*, is shown. Loss of Zivi leads to a strong reduction in the amount of *vasa* positive cells.

(E) Caspase-3 staining of wild-type and *zivi(hu2479/hu2479)* animals at 21 days of development is shown. The developing germline is indicated. Wild-type gonads ($n = 3$) do not show apoptosis at this point in time, whereas the mutant gonads ($n = 3$; brown cells) do.

Zebrafish piRNAs Are Present in Both Male and Female Germline

In mammals, Piwi proteins interact with a new class of germ-cell-restricted small RNAs (~26–30 nucleotides long) called piRNAs. We therefore asked if a similar population of RNAs exists in zebrafish germ cells. Indeed we found that a population of small RNAs, ~26–30 nucleotides long, could be visualized simply by SYBRGold staining (Figure 3A). However, in contrast to mammals, not only testis but also ovary expresses these small RNA molecules, albeit at lower levels. In no other tissue have we seen a similar population. We isolated the approximately 28 nucleotide population from both ovary and testis and performed large-scale sequencing. The results are summarized in Table 1.

To confirm that the sequences we obtained correspond to RNAs expressed specifically in gonads, we performed northern blot analysis. All probes that gave a detectable

signal on a northern blot produced a gonad-specific signal of the predicted length (approximately 28 nucleotides; Figures 3C and S3A). Furthermore, these molecules are sensitive to treatment with RNaseA (Figure S3B), and fractionation of ovarian extracts over both a size-exclusion column and an ion-exchange column shows perfect cofractionation of Zivi and small RNA, strongly suggesting that these RNAs are bound by Zivi (Figures 3E–3F). We will therefore refer to these RNAs as piRNAs.

Zebrafish piRNAs have a strong U bias at the most 5' position (Figure S4A) and display a Gaussian length distribution with a single peak around 26–28 nucleotides (Figure 3B). When the surrounding sequences of the potential small-RNA-producing loci were analyzed for the potential to produce miRNA-like precursor molecules, it was clear that the vast majority of the piRNA sequences (approximately 94%) were most likely not derived from such hairpin precursor molecules (not shown). In addition, piRNAs

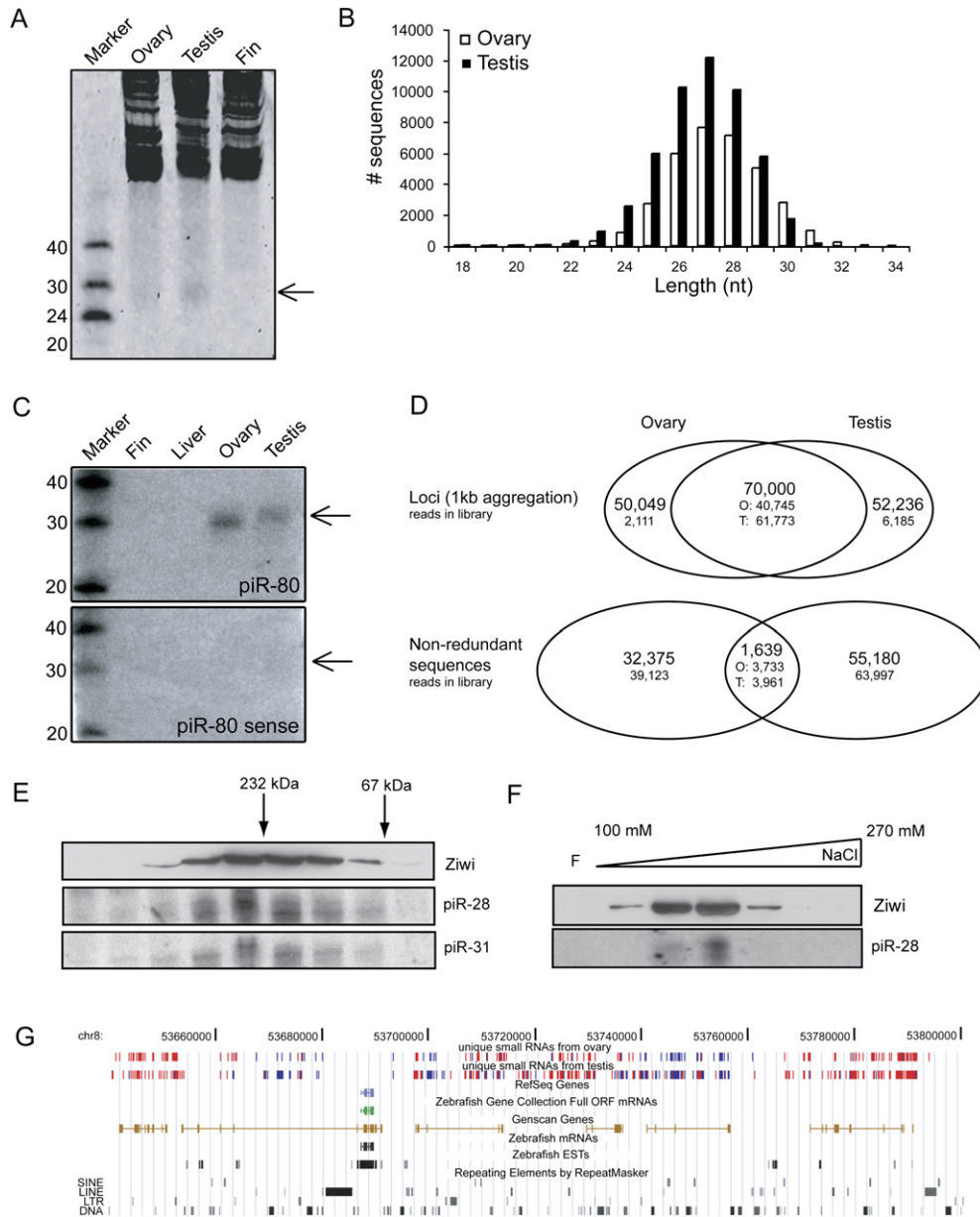


Figure 3. Zebrafish piRNAs in Ovary and Testis

(A) SYBRGold staining of 20 µg total RNA is shown. A 28 nt band is visible in testis and ovary but not in fin.

(B) Length distribution of cloned small RNAs from zebrafish ovary and testis is shown.

(C) Ovary- and testis-specific detection of small RNAs by northern blotting is shown. Sense indicates a probe with same sequence as the cloned piRNA sequence.

(D) Graphic representation of the overlap between ovary and testis libraries. In the overlap regions the number of ovary (O)- and testis (T)-derived reads that contribute to the total number of loci or nonredundant sequences are indicated. Loci are defined as regions where two different piRNAs are maximally 1 kb apart.

(E) Ziwi cofractionates with piRNAs on a size exclusion column. Upper panel shows western blot for Ziwi. Lower panels show northern blots for piR-28 and piR-31.

(F) Ziwi cofractionates with piRNAs on a Resource S column eluted with a salt gradient from 100 mM to 1 M NaCl. Upper panel shows western blot for Ziwi. Lower panel shows northern blot for piR-28.

(G) A view from the UCSC browser displays a part of chromosome 8. Red bars depict piRNA reads originating from the positive strand, and blue bars depict reads from the negative strand. Other features of this region are indicated in the figure.

Table 1. Identified RNA Species

RNA Class	# Reads Ovary		# Reads Testis	
		%		%
Known miRNA	391	1	797	1
Noncoding RNA	1,137	3	1,117	2
piRNA	42,856	96	67,958	97
Nonrepeat piRNA	21,241	50 ^a	45,899	68 ^a
Simple repeat piRNA	7,074	16 ^a	7,922	11 ^a
Repeat piRNA	14,541	34 ^a	14,137	21 ^a
Nonrepeat; intergenic	18,010	85 ^b	37,645	82 ^b
Nonrepeat; exon	1,599	7 ^b	4,786	10 ^b
Nonrepeat; intron	1,632	8 ^b	3,468	8 ^b
LTR	9,385	65 ^c	8,219	58 ^c
LTR +strand	2,225	24	3,387	41
LTR -strand	7,160	76	4,832	59
NonLTR	1,677	18 ^c	2,114	15 ^c
NonLTR +strand	934	34	942	47
NonLTR -strand	1,743	66	1,172	53
DNA	1,813	12 ^c	3,201	23 ^c
DNA +strand	884	49	1,431	45
DNA -strand	932	51	1,770	55
GypsyDR1 +strand	102	8	204	21
GypsyDR1 -strand	1,242	92	787	79
GypsyDR2 +strand	33	3	89	22
GypsyDR2 -strand	1,039	97	322	78

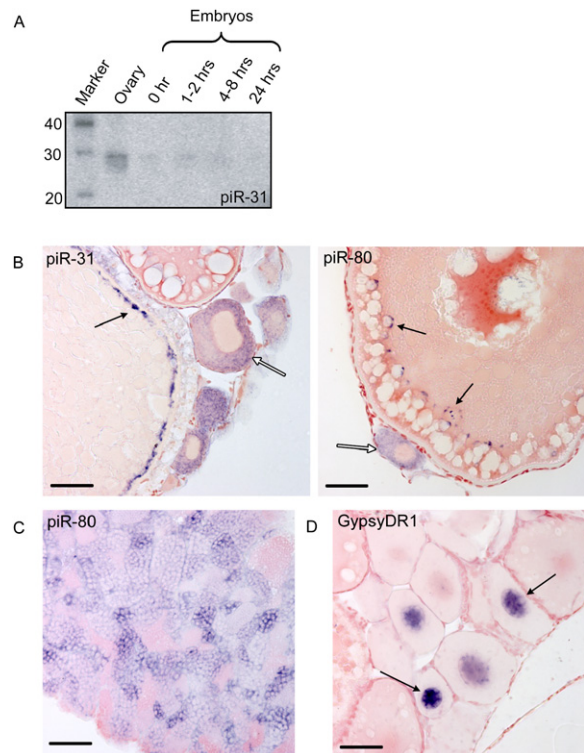
piRNAs are split into three categories: Nonrepeat, simple repeat, and repeat. Nonrepeat piRNAs have been split into three groups: intergenic, intronic, and exonic. The repeat-associated piRNAs have been split into three categories: those matching to LTR, nonLTR, and DNA transposons. For each class it is indicated how many piRNAs map to the respective element and to which strand with regard to the transposon. Two LTR elements are shown in detail (GypsyDR1 and GypsyDR2; numbers reflect summary of all GypsyDR1 and DR2 elements in the genome). Noncoding RNA: tRNA, rRNA, snRNA, and snoRNA.

^a Percentages are given with respect to total piRNA collection.

^b Percentages are given with respect to nonrepeat-associated piRNAs.

^c Percentages are given with respect to repeat-associated piRNAs.

display a very strong strand asymmetry (Figures 3C and 3G). Both ovary and testis libraries are not saturated; approximately 90% of the sequences have been read only once. However, the vast majority of the ovary- and testis-derived sequences derive from the same loci (Figures 3D and S5). This most likely indicates that piRNAs are not produced as specific sequences but are representatives of discrete loci in the genome. Interestingly, when piRNA densities between ovary and testis are compared,

**Figure 4. piRNA Expression**

(A) Northern blot for piRNA piR-31 at various developmental stages is shown.

(B) shows piR-31 and piR-80 in situ hybridization on ovary. Open arrows indicate stage I oocytes, displaying staining in the cytoplasm. Closed arrows indicate granules along the cortex of stage III/IV oocytes. Scale bars are 50 μm.

(C) piR-80 in situ hybridization on testis is shown. Cytoplasmic staining is observed in all stages, including premeiotic stages, except for sperm.

(D) GypsyDR1 in situ hybridization on ovary is shown. Nuclear staining is observed in stage I oocytes and rapidly fades in older stages.

more than 200 loci that have a 10-fold overrepresentation in ovary compared to testis are observed, compared to only seven regions that are more abundant in the testis library (Table S3). All piRNA sequences are deposited at <http://www.ncbi.nlm.nih.gov/geo/> under series number GSE7131.

piRNA Expression

Northern blot analysis revealed that piRNAs can be transmitted maternally (Figure 4A). To examine the expression of piRNAs in more detail we performed in situ hybridizations using LNA oligonucleotides as probes. In summary, piRNA expression largely mirrors *ziwi* expression: in ovary, piRNAs are found in the cytoplasm of primary oocytes and in maturing oocytes become restricted to the cortex (Figure 4B). At this time piRNAs are present in granules much like the granules we observe for *Ziwi*. In oogonia and PGCs we do not see expression of piRNAs while *Ziwi* is present. This could indicate that *Ziwi* may have

functions independent of piRNAs. In testis we find cytoplasmic expression in all stages except sperm (Figure 4C). The absence of nuclear staining most likely is significant, as our protocols do allow the detection of nuclear RNA (Figure 4D).

Genomic Distribution of piRNAs

Many of the piRNA sequences map to sequences that are annotated as a transposon (34% in the ovary and 21% in the testis library). Of the nonrepetitive sequences more than 80% map to intergenic regions. Genes associated with piRNAs do not show obvious relationships as assessed by GO terms (Table S4). All sequences, both repetitive and nonrepetitive, derive from the same clusters (Figures S5A–S5B) that are widely distributed over the genome. Within clusters we find stretches of sequence up to several kilobases that are represented by piRNAs from only one strand, flanked by regions that are represented by piRNAs from the other strand (Figure 3G). Interestingly, unlike piRNA clusters in mammalian testis (Aravin et al., 2006; Girard et al., 2006), strand polarity in zebrafish switches back and forth: of the 682 loci that are defined by the presence of ten or more uniquely mapping piRNAs with a spacing of maximally 1 kilobase, 537 switch strand polarity more than once (Table S5).

Many zebrafish piRNAs derive from repetitive sequences; this is in stark contrast to mammalian piRNAs that are significantly biased toward nonrepetitive sequences (Aravin et al., 2006; Girard et al., 2006). When analyzed genome-wide, a correlation between piRNA density and retroelements can be observed. As an example we show the transposon density of chromosome 4 together with the piRNA density (Figure 5A). This correlation can be seen whether or not we represent the piRNAs weighted by the number of times they map to the genome. Many piRNAs map to several loci in the genome. To visualize the areas that are most likely generating these repetitive piRNAs, we assign a weight to each piRNA reflecting the number of times it maps to the genome. Some piRNA peaks disappear when we weigh the piRNAs. These loci most likely represent regions with mutated and presumably inactive piRNA loci; they show homology to repeat derived piRNAs but to a small subset only. This analysis also reveals that the piRNAs that map to only one locus display a similar distribution pattern compared to the piRNAs that map to repeated elements. Most likely this indicates that many of these piRNAs map only once because they map to a uniquely mutated version of a repetitive sequence.

When analyzed in more detail it becomes evident that piRNAs preferentially derive from LTR elements; approximately 8% of all transposon-related repeats in the genome correspond to LTR elements, whereas we find that approximately 60% of the repeat-derived piRNAs stem from LTR elements (Table 1). We also detect a strong strand bias for ovarian piRNAs and, to some extent, testicular piRNAs with regard to the orientation of nonDNA transposons, with piRNAs mainly deriving from the anti-

sense strand (Table 1). This effect is particularly strong for the GypsyDR1 and GypsyDR2 elements as shown in Figures 5B–5C and Table 1. When we plot all the piRNAs that match an LTR transposon or fragments thereof against a consensus sequence of the complete element, a characteristic phasing pattern arises: peaks of antisense piRNAs are seen every 200–300 nucleotides. As examples we show this for GypsyDR1 and GypsyDR2 (Figures 5D–5E), but we also see this for other LTR elements like Ngaro. The patterns from ovary- and testis-derived sequences are very similar.

piRNAs Have a 5' Phosphate and a Modified 3' End

Next, we analyzed the chemical structures of both the 5' and 3' ends of the zebrafish piRNAs. Phosphatase treatment of piRNAs leads to a reduction of mobility through a 12% denaturing polyacrylamide sequencing gel, and this can be restored to the original mobility by rephosphorylation of the 5' end (Figure 6A). Furthermore, piRNAs can be efficiently ligated to a 17 nucleotide linker with both 5' and 3' hydroxyl groups using T4 RNA ligase. Both experiments indicate that a monophosphate group has to be present at the 5' end (Figure 6B). To probe the 3' end of piRNAs, we performed NaIO₄-mediated oxidation followed by a β-elimination reaction. When the last nucleotide of an RNA molecule contains both 2' and 3' OH groups, this treatment removes the most 3' base, leaving a 3' phosphate on the remainder of the molecule. This results in an RNA species that has an apparent mobility of two fewer nucleotides compared to the original RNA (Yu et al., 2005). Three different piRNAs are resistant to this reaction (Figures 6A and S6), while within the same samples the miRNA let-7a is completely converted, indicating that either the 2' or the 3' OH group of the most 3' nucleotide of piRNAs is modified. Identical results are obtained for mouse and rat piRNAs (Figure S6), indicating that 3' end modification is a conserved feature of piRNA biogenesis. The tested piRNAs represent sequences with all four possible bases as last nucleotide (see Supplemental Experimental Procedures), indicating that the modification is not base specific. We next probed the identity of the 3' modification. For this we used rat piRNAs, as we could not obtain enough material to perform the experiment on zebrafish. After degrading purified piRNAs (Figure 6C) into nucleosides using RNaseOne we analyzed the chemical composition using HPLC and mass spectrometry, resulting in the identification of a 2'-O-Methyl modification on a fraction of the A nucleosides (Figures 6D, 6E and S7). Because of technical reasons we cannot faithfully detect modified C, G, and U in our samples (see Supplemental Experimental Procedures), but by extrapolation we expect that 3' terminal Cs, Gs, and Us on piRNAs will also carry a 2'-O-Methyl.

Genetic Requirements of piRNAs

We addressed the genetic requirements for piRNA production through the use of mutants or animals carrying a morpholino-induced phenotype (Figure 6F). First, in the

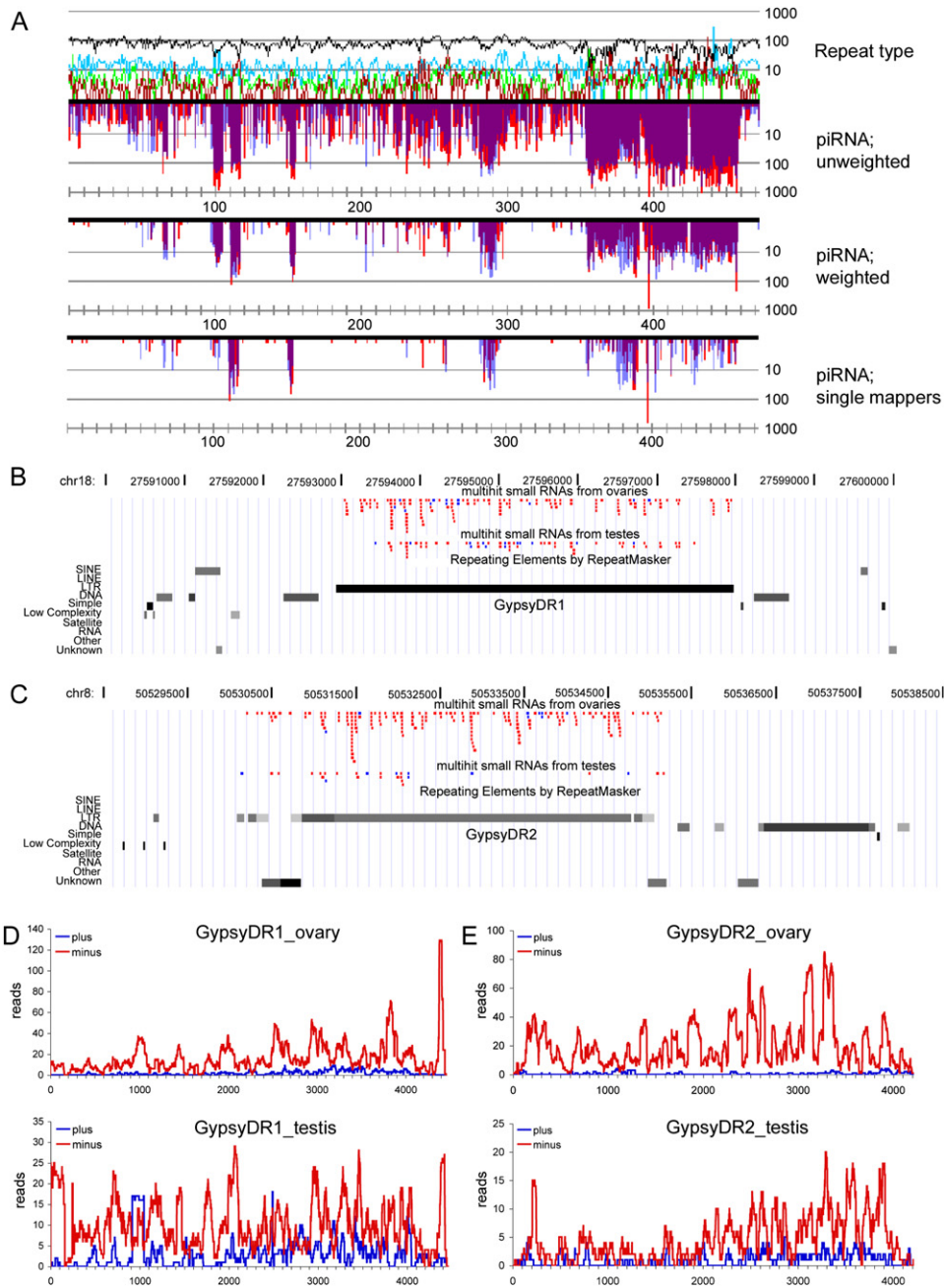


Figure 5. Transposon-Derived piRNAs

(A) Transposon density and piRNA density are shown along chromosome 4. Above the chromosome different types of transposons are indicated: black-DNA; green-LINE; Blue-SINE; and Red-LTR. The piRNAs are indicated as red (ovary) and blue (testis) bars below the chromosome in three different representations. Top row shows all piRNAs, unweighted. Middle row shows all piRNAs, weighted (see text). Lower row shows piRNAs that map to a single locus. Bin size is 100 kb.

(B) shows a locus on chromosome 18 containing a full length GypsyDR1 element and showing the distribution of piRNAs. Red indicates (+)strand, and blue indicates (-)strand of the chromosome. This particular element is oriented from right to left.

(C) A locus on chromosome 8 containing a full length GypsyDR2 element, showing the distribution of piRNAs, is shown. Red indicates (+)strand, and blue indicates (-)strand of the chromosome. This particular element is oriented from right to left.

(D) Distribution of all GypsyDR1 piRNAs is shown across the consensus sequence of the element. Red line indicates piRNAs corresponding to the (-)strand of the element. Blue line indicates piRNAs corresponding to the (+)strand of the element.

(E) Distribution of all GypsyDR2 piRNAs across the consensus sequence of the element is shown. Red line indicates piRNAs corresponding to the (-)strand of the element. Blue line indicates piRNAs corresponding to the (+)strand of the element.

homozygous *ziwi* mutant testis we do not detect piRNAs. The same is true for testis isolated from animals that have been treated with a morpholino targeting the *dead-end* gene that results in the complete loss of germ cells (Weidinger et al., 2003). Consistent with our piRNA-expression data (Figures 4B and 4C), these results indicate that zebrafish piRNAs are expressed in the germ cells. We see no effect of the *ziwi*(N686K) missense mutation. This may indicate that the N686K mutation affects piRNA function rather than piRNA synthesis. Next, we tested the requirement for Dicer through the use of animals that carry homozygous *dicer* mutant germ cells in a surrounding of *dicer* wild-type cells (Giraldez et al., 2005). In testes isolated from these animals we detect normal levels of piRNAs, strongly suggesting that piRNA biogenesis is independent of Dicer.

DISCUSSION

Ziwi Function in the Germline

Effects of Piwi mutations on germline development differ among species. In *Drosophila*, a role in both the somatic germline as well as in the germ cells has been identified (Cox et al., 1998, 2000). In mammals, *miwi* and *mili* knockout animals show defects specifically in male germ cells, consistent with their testis-specific expression (Deng and Lin, 2002; Kuramochi-Miyagawa et al., 2004). Sperm cell differentiation is halted at different meiotic stages, coincident with the expression pattern of these two proteins. Our data show that the loss of Piwi function in another vertebrate, the zebrafish, affects germ cells during earlier development, triggering apoptosis in pre-meiotic cells, most likely in a cell-autonomous manner. Partial loss of Ziwi permits the survival of germ cells but results in elevated levels of apoptosis in adult germ cells. Whether the apoptosis of the adult germ cells is mechanistically related to the apoptosis we observe in the developing gonad is not clear. It should be noted that we do not know whether loss of Ziwi triggers apoptosis directly or indirectly and whether this is piRNA dependent or independent. We clearly observe Ziwi expression in cells that lack piRNAs (for example, the PGCs), suggesting that Ziwi indeed has piRNA independent functions. At present we have no good indications what these functions might be. When piRNA-dependent functions of Ziwi are involved, transposon-inflicted DNA damage could be responsible for the induction of apoptosis. However, as many piRNAs are not transposon related, there may well be other reasons for *ziwi* mutant cells to go into apoptosis.

Germ Granules

The intracellular localization of Ziwi and piRNAs in distinct granules localized to specific sites in the cytoplasm is typical of factors that have been implicated in germ cell specification in various species (Gruidl et al., 1996; Rongo et al., 1997). The precise function of these granules is not known, but they share many components with cytoplasmic bodies called P bodies in somatic cells. These bodies

have been implicated in RNAi- and miRNA-mediated silencing but have also been shown to be able to release mRNAs into the actively translating pool of mRNAs (Bregues et al., 2005), suggesting that they may act as mRNA-storage particles. In mice, MIWI has been localized to the chromatoid body (Kotaja et al., 2006), a large granular structure only present in sperm cells close to the end of their differentiation pathway. It has been suggested that the chromatoid body may have a role in scavenging transcripts that come from the nucleus in these transcriptionally inactive cells (Kotaja et al., 2006). Taken together, it seems that these germ-cell-specific structures may be required for a number of processes, ranging from the quenching of residual transcription to the regulation of translational activity of maternal mRNAs, and Piwi-like proteins seem well suited to carry out at least a number of these tasks. Given the link between Ziwi and transposable elements (see below) we can add that germ granules may be involved in preventing unwanted activity of transposable elements in early embryos.

Piwi: Cytoplasmic or Nuclear?

What is the subcellular compartment in which Piwi proteins are active? Steady-state levels of Ziwi and piRNAs are highest in the cytoplasm, indicating that if Ziwi is acting in the nucleus, either only a small fraction of Ziwi must be doing so or the nuclear localization is very transient. In rat, RIWI has been found associated with piRNAs and another protein, RecQ (Lau et al., 2006), leading to the suggestion that this complex may function at the DNA level. Interestingly, in *Drosophila* Piwi has been found to be both nuclear and cytoplasmic (Cox et al., 2000), and it has been shown that Piwi is involved in the nuclear long-range organization of transcriptionally repressed loci (Grimaud et al., 2006). On the other hand, MIWI and associated piRNAs have been found associated with ribosomes, suggesting a function in translational regulation (Grivna et al., 2006b).

piRNAs and Transposable Elements

Through our sequencing we have found that the majority of zebrafish piRNAs are derived from discrete genomic clusters. In contrast to mammalian piRNAs, a large fraction of those identified in fish map to transposable elements, in particular LTR elements. For all the retroelement-derived ovarian piRNAs we analyzed, we find a very strong bias to the minus strand of the element. This strand bias is also present in the testis library, although it is less pronounced, and is not observed for piRNAs matching to DNA transposons, perhaps reflecting the activity of these elements, as no active DNA transposon has yet been identified in vertebrate genomes. If a self-amplifying loop is involved in piRNA biogenesis (see “Biogenesis of piRNAs” below), then piRNAs derived from DNA transposons may reflect a “start-up” population that would trigger the massive production of antisense piRNAs if an element is active. Consistent with this idea is the fact that transposon-derived piRNAs are strongly depleted for DNA transposons: only 10%–20% of the repeat-derived

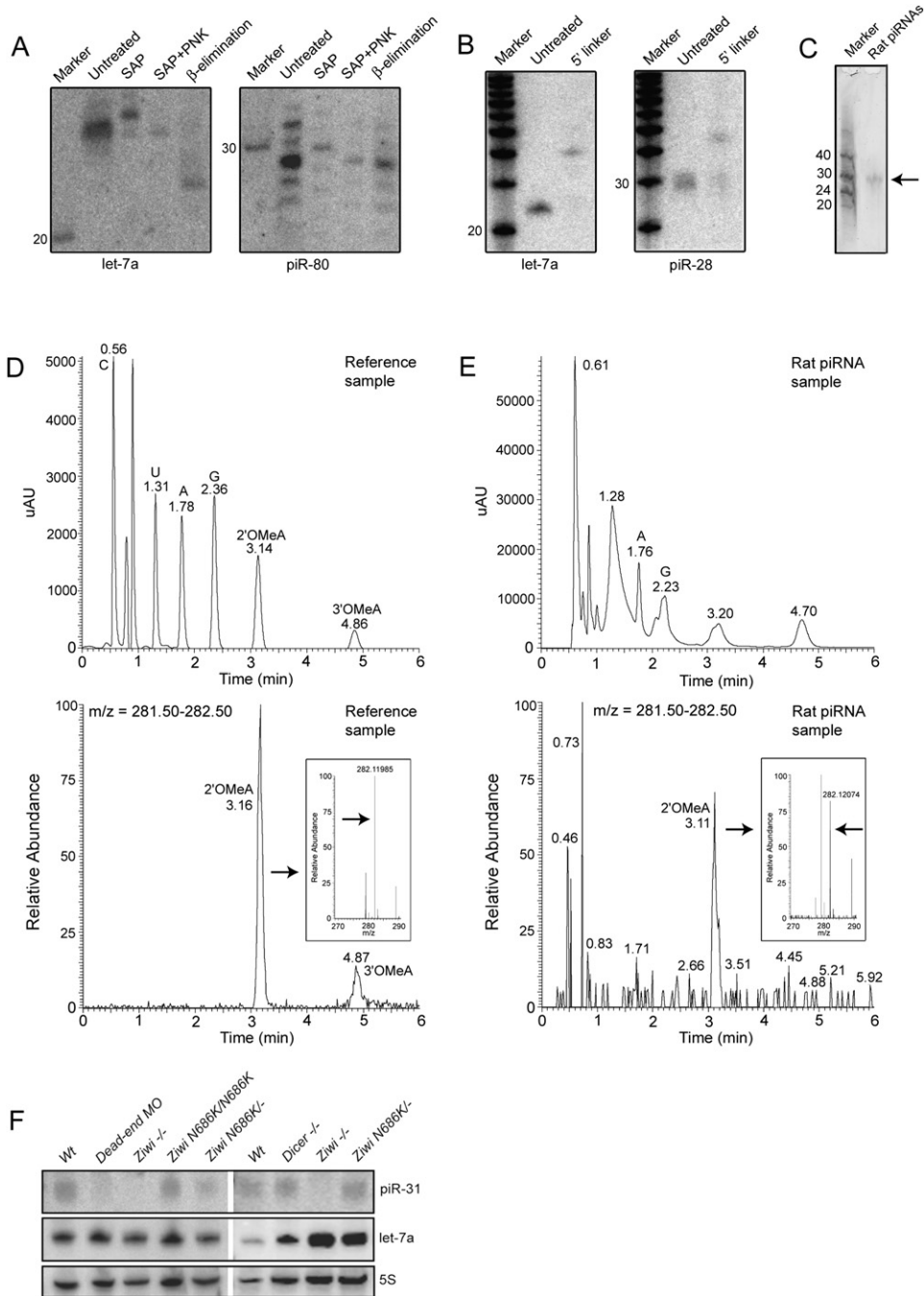


Figure 6. Biochemical and Genetic Analysis of piRNAs

(A) Left panel shows a northern blot for let-7a. Samples are treated with Shrimp Alkaline Phosphatase (SAP), SAP+ polynucleotide kinase (PNK), and NaIO₄ oxidation followed by β-elimination. The right panel shows the same blot probed for piR-80.

(B) Ligation of a 17 nt linker with both 5' and 3' hydroxyl groups to both let-7a and piR-28 is shown.

(C) Purified rat piRNA is shown. Approximately 0.3% of the purified product was run on a gel and stained with SYBRGold.

(D) LC/MS characterization of a mix of synthetic C, A, U, G, 2'-OMeC, 3'-OMeC, 2'-OMeA, and 3'-OMeA is shown. In the top graph UV intensity is plotted versus time. In the lower graph the presence of molecules with an m/z in the range of OMeA (m/z = 282.12) is plotted versus time, revealing peaks at the retention times (RT) of 2' and 3'-OMeA. The inset shows high resolution m/z determination (RT = 3.06–3.25), with an arrow pointed at the exact mass of 2'-OMeA. Numbers in the graph indicate RT of indicated peak.

(E) Similar experiment as in (D) but now with nucleosides derived from rat piRNAs. Two UV peaks are observed around the RT of 2' and 3'-OMeA. The peak overlapping with 2'-OMeA contains molecules with the mass of OMeA (m/z = 282.12 at RT = 3.05–3.22; lower graph and inset). This species is present in the left shoulder of the UV peak at RT = 3.20. Note that most of the UV signal of the peak at RT = 3.20 does not come from 2'-OMeA. The UV

piRNAs stem from DNA transposons, while they make up more than 70% of all transposons in the zebrafish genome. In comparison, roughly 60% of all repeat-derived ovarian piRNAs derive from LTR elements, while they comprise only 8% of all transposons. This trend also holds true for many, but not all, individual elements analyzed (Table S6). Differences between the ovary- and testis-derived libraries may similarly be explained by differential activity of (transposable) elements between these two tissues.

A curious feature of transposon-derived piRNAs is that they show a striking periodicity. This is shown for two Gypsy elements in Figure 5, but we observe comparable patterns for other elements, including some DNA transposons. We observe very similar patterns for both ovary- and testis-derived sequences, suggesting that this periodicity reflects some unidentified biological process, rather than being the result of experimental artifacts. The cause of this periodicity may lie either in the transcription of these loci, the processing of the resulting transcripts, or the stability of final piRNAs. At present we have no good way of discriminating between these possibilities. It should also be noted that in *Drosophila* no periodicity for piRNAs has been observed in ovary (G.J.H., J. Brennecke, and A. Aravin, unpublished data).

The correlation between piRNAs and retroelements indicates that these RNAs may have a role in their activity, as has been suggested for *Drosophila* rasiRNAs and Piwi-associated RNAs (Aravin et al., 2003; Saito et al., 2006). A recent study by Brennecke et al. (2007) shows that piRNA-generating clusters in *Drosophila* map to known mutator loci that have genetically been linked to transposon activity, providing genetic support for a link between transposon silencing and piRNAs. These results markedly differ from the mammalian situation, where piRNAs seem to be overrepresenting nonrepetitive DNA (Aravin et al., 2006; Girard et al., 2006). However, some retrotransposon-derived small RNAs have been isolated from mouse oocytes (Watanabe et al., 2006), and Carmell et al. (2007) show that mutations in MIWI2 lead to activation of transposons, indicating that an RNA-based germline defense mechanism may be a more general phenomenon in vertebrates. In our system we have not yet seen an activation of transposable elements, either in 2-week-old gonads in *ziwi* null mutants or in testis from adult *ziwi* hypomorphic mutants. These experiments are, however, hampered by the fact that germ cells die when *Ziwi* function is compromised, possibly preventing proper analysis of transposon activity. In addition, the second *piwi*-like gene, *zili*, is still functional in these mutants, and this gene may in some aspects act redundantly with *ziwi*.

Biogenesis of piRNAs

The biogenesis of piRNAs appears to be different from that of siRNAs and miRNAs. First, piRNAs are asymmetric: only one strand of a particular sequence is represented. This is very atypical of siRNAs, where both strands can usually be identified, albeit often in unequal amounts (Schwarz et al., 2003), indicating that piRNAs may be derived from single-stranded RNA. The strand switching we observe most likely reflects the presence of two transcripts meeting head-on or starting from a divergent promoter. Recently, 21U RNAs have been described in *C. elegans* (Ruby et al., 2006). These short RNAs contain very precisely defined 5' ends, and each appears to be made from its own promoter. Given the fact that we observe considerable 5' variability, we think this is an unlikely scenario for the transcription of zebrafish piRNAs.

Second, all piRNAs tested so far—nine in total, in zebrafish as well as in mouse and rat—are resistant to periodate treatment, indicating a modified 2' or 3' hydroxyl group on the most 3' base. Consistent with these findings, we detect the presence of 2'O-MeA in rat piRNAs. Assuming that the tested piRNAs are representative for most or all piRNAs, it is likely that vertebrate piRNAs carry a 2'O-Methyl modification at their 3' ends. Plant, but not animal, miRNAs carry the same modification, and this is placed on the miRNA by an enzyme named HEN1. The role of this modification is not known, but in plants lacking HEN1, miRNA levels drop (Yu et al., 2005), indicating that this modification may be required for stability. Animal genomes do encode proteins homologous to HEN1, so it will be interesting to analyze the effect of these homologs on piRNA abundance and/or function.

Third, we present genetic evidence that Dicer is not involved in the generation of piRNAs. Consistent with this, germ cells lacking Dicer develop normally (Giraldez et al., 2005), in contrast to *ziwi*-deficient germ cells. In theory, it is possible that somatically expressed Dicer is confounding our results. However, this hypothesis would have to postulate an interaction between germ cells and somatic germline tissue resulting in the somatic expression of piRNAs that are then transported into the germ cells. Based on piRNA expression data we prefer the simpler interpretation that Dicer is not involved in piRNA generation.

As discussed above, zebrafish piRNAs that correspond to LTR elements are derived mainly from the antisense strand. A similar bias has been reported in *Drosophila* (Gunawardane et al., 2007; Vagin et al., 2006; Brennecke et al., 2007). However, additional observations regarding piRNAs that correspond to the sense strands of transposons were made (Gunawardane et al., 2007; Brennecke et al., 2007). These reside mainly in Ago3 complexes

peak around the RT of 3'-OMeA contains no species with a molecular weight of 3'-OMeA (not shown). Coinjection with synthetic 2' and 3'-OMeA confirms these results (Figure S7).

(F) Northern blot analysis of piRNA expression is shown in various mutant backgrounds. Upper panel shows a northern blot for piRNA piR-31. The same blot was probed for miRNA let-7a (middle panel) and 5S RNA (lower panel). Note that let-7a is expressed in the somatic germline (not shown), so disruption of *dicer* in the germ cells has no effect on let-7a processing.

and lack a U bias at their 5' ends. Coupling this observation with the fact that many Ago3-bound piRNAs are enriched for A at position 10 and show complementarity to antisense piRNAs in their first 10 nucleotides (which are associated with Aub), a biogenesis mechanism is proposed in which cleavage by Piwi-family proteins can create the 5' ends of piRNAs (Gunawardane et al., 2007; Brennecke et al., 2007). Moreover, Brennecke and colleagues propose an amplification loop wherein sense and antisense transposon piRNAs act on piRNA clusters and dispersed transposon copies, respectively, to increase the abundance of piRNAs targeting specific elements. Notably, in zebrafish, the collective subset of piRNAs that match sense strands of all GypsyDR1 and GypsyDR2 loci also lack a marked U bias. Instead, they are enriched for A at position 10 (Figures S4B–S4C), exactly as seen for *Drosophila* Ago3-bound RNAs. This suggests evolutionary conservation not only of piRNA biogenesis strategies but also of the biochemical pathways used for transposon control. It remains to be seen whether zebrafish also compartmentalize sense and antisense piRNAs in discrete Piwi complexes.

EXPERIMENTAL PROCEDURES

Detailed descriptions of all the procedures can be found in the [Supplemental Data](#).

Zebrafish Strains and Genetics

Zebrafish were kept under standard conditions (Westerfield, 1993) and staged according to Kimmel et al. (1995). Zebrafish mutants were derived from ENU mutagenized libraries using target-selected mutagenesis as described (Draper et al., 2004; Wienholds et al., 2003). Fish with mutant alleles (*ziwi* hu2479/+, Q543STOP; *ziwi* fh219/+, R561STOP; *ziwi* hu2410/+, N686K; *ziwi* fh221/+, Y728STOP; and *ziwi* fh222/+, I694N) were outcrossed against wild-type fish (*AB or TL) and subsequently incrossed against each other to obtain heteroallelic or homozygous offspring. *Tg(PGC:GFP)* have been described before (Blaser et al., 2006; Krovel and Olsen, 2002). Details of genotyping are provided in the [Supplemental Data](#).

Ziwi Antibody

Ziwi antibodies were raised in rabbits against the synthetic peptide EGQLVGRGRQKPAPGC. Antisera were subsequently affinity purified (Eurogentec).

piRNA Cloning

Zebrafish organs were frozen in liquid nitrogen and powdered, and total RNA was isolated using Trizol (Invitrogen). Twenty micrograms of total zebrafish ovary or testis RNA was separated by 15% denaturing polyacrylamide gel and visualized by SYBRGold staining, and small RNAs of ~24–40 nt were gel purified. These were cloned and sequenced as described before (Girard et al., 2006). Sequences are available through <http://www.ncbi.nlm.nih.gov/geo>, series GSE7131.

Sequence Analysis

Adaptor sequences were trimmed from 454-generated data using custom scripts. Resulting inserts were mapped to the zebrafish genome (Zv6 assembly, March 2006) using megablast program (Zhang et al., 2000) and blast parser from bioperl (Stajich et al., 2002). Genomic annotations of mapped reads were retrieved from Ensembl database (v. 41, October 2006) using Perl API provided by Ensembl (Birney et al., 2006). Sequences were grouped into families using blastclust

program from the NCBI toolkit (<ftp://ftp.ncbi.nih.gov/blast>) with the word parameter set to 16. Nucleotide-frequency graphs were generated by WebLogo software (Crooks et al., 2004).

Analysis of piRNA Chemical Structure

Analysis of the 3' end and 5' end structures was done as described previously (Vagin et al., 2006). Rat piRNAs were purified by running low-molecular-weight RNA from two testes over a HiLoad 16/60 superdex 200 column. Peak fractions were precipitated and rerun over a superdex 200 10/300GL column. Peak fractions were degraded with RNaseOne and treated with SAP, then analyzed using LC/MS.

Supplemental Data

Supplemental Data include Results and Discussion, Experimental Procedures, References, six tables, and seven figures and can be found with this article online at <http://www.cell.com/cgi/content/full/129/1/69/DC1/>.

ACKNOWLEDGMENTS

We thank Dr. Rüdiger Schultz for help in analyzing testis slides; Dr. Edwin Cuppen, Ewart de Bruijn, Thomas Donn, and Jessica Mullenberg for assistance in screening for zebrafish mutants; and Eugenel Espiritu for technical assistance. We thank Professor Gijs van der Marel for discussion. Male zebrafish carrying *dicer* mutant germ cells were provided by Dr. Antonio Giraldez. Drs. Karin Dumstrei and Lisbeth Olsen provided transgenic animals. Antibodies to zebrafish Vasa were kindly provided by Dr. Holgar Knaut. This work was supported by the European Science Foundation under the EUROCORES Programme EuroDYNA, through contract number ERAS-CT-2003-980409 of the European Commission, DG Research, FP6 (R.F.K.), and a VIDJ fellowship from the Dutch Organisation for Scientific Research (NWO; R.F.K.).

Received: November 3, 2006

Revised: January 24, 2007

Accepted: March 20, 2007

Published: April 5, 2007

REFERENCES

- Aravin, A., Gaidatzis, D., Pfeffer, S., Lagos-Quintana, M., Landgraf, P., Iovino, N., Morris, P., Brownstein, M.J., Kuramochi-Miyagawa, S., Nakano, T., et al. (2006). A novel class of small RNAs bind to MILI protein in mouse testes. *Nature* 442, 203–207.
- Aravin, A.A., Lagos-Quintana, M., Yalcin, A., Zavolan, M., Marks, D., Snyder, B., Gaasterland, T., Meyer, J., and Tuschl, T. (2003). The small RNA profile during *Drosophila melanogaster* development. *Dev. Cell* 5, 337–350.
- Bernstein, E., Caudy, A.A., Hammond, S.M., and Hannon, G.J. (2001). Role for a bidentate ribonuclease in the initiation step of RNA interference. *Nature* 409, 363–366.
- Birney, E., Andrews, D., Caccamo, M., Chen, Y., Clarke, L., Coates, G., Cox, T., Cunningham, F., Curwen, V., Cutts, T., et al. (2006). Ensembl 2006. *Nucleic Acids Res.* 34, D556–D561.
- Blaser, H., Reichman-Fried, M., Castanon, I., Dumstrei, K., Marlow, F.L., Kawakami, K., Solnica-Krezel, L., Heisenberg, C.P., and Raz, E. (2006). Migration of zebrafish primordial germ cells: a role for myosin contraction and cytoplasmic flow. *Dev. Cell* 11, 613–627.
- Braat, A.K., Zandbergen, T., van de Water, S., Goos, H.J., and Zivkovic, D. (1999). Characterization of zebrafish primordial germ cells: morphology and early distribution of vasa RNA. *Dev. Dyn.* 216, 153–167.

- Bregues, M., Teixeira, D., and Parker, R. (2005). Movement of eukaryotic mRNAs between polysomes and cytoplasmic processing bodies. *Science* 310, 486–489.
- Brennecke, J., Aravin, A.A., Stark, A., Dus, M., Kellis, M., Sachidanandam, R., and Hannon, G.J. (2007). Discrete small RNA-generating loci as master regulators of transposon activity in *Drosophila*. *Cell* 128, 1089–1103.
- Carmell, M.A., Girard, A., van de Kant, H.J.G., Bourc'his, D., Bestor, T.H., de Rooij, D.G., and Hannon, G.J. (2007). MIWI2 Is Essential for Spermatogenesis and Repression of Transposons in the Mouse Male Germline. *Dev. Cell*, in press.
- Carmell, M.A., Xuan, Z., Zhang, M.Q., and Hannon, G.J. (2002). The Argonaute family: tentacles that reach into RNAi, developmental control, stem cell maintenance, and tumorigenesis. *Genes Dev.* 16, 2733–2742.
- Cox, D.N., Chao, A., Baker, J., Chang, L., Qiao, D., and Lin, H. (1998). A novel class of evolutionarily conserved genes defined by piwi are essential for stem cell self-renewal. *Genes Dev.* 12, 3715–3727.
- Cox, D.N., Chao, A., and Lin, H. (2000). piwi encodes a nucleoplasmic factor whose activity modulates the number and division rate of germline stem cells. *Development* 127, 503–514.
- Crooks, G.E., Hon, G., Chandonia, J.M., and Brenner, S.E. (2004). WebLogo: a sequence logo generator. *Genome Res.* 14, 1188–1190.
- Deng, W., and Lin, H. (2002). miwi, a murine homolog of piwi, encodes a cytoplasmic protein essential for spermatogenesis. *Dev. Cell* 2, 819–830.
- Draper, B.W., McCallum, C.M., Stout, J.L., Slade, A.J., and Moens, C.B. (2004). A high-throughput method for identifying N-ethyl-N-nitrosourea (ENU)-induced point mutations in zebrafish. *Methods Cell Biol.* 77, 91–112.
- Elbashir, S.M., Lendeckel, W., and Tuschl, T. (2001). RNA interference is mediated by 21- and 22-nucleotide RNAs. *Genes Dev.* 15, 188–200.
- Giraldez, A.J., Cinalli, R.M., Glasner, M.E., Enright, A.J., Thomson, J.M., Baskerville, S., Hammond, S.M., Bartel, D.P., and Schier, A.F. (2005). MicroRNAs regulate brain morphogenesis in zebrafish. *Science* 308, 833–838.
- Girard, A., Sachidanandam, R., Hannon, G.J., and Carmell, M.A. (2006). A germline-specific class of small RNAs binds mammalian Piwi proteins. *Nature* 442, 199–202.
- Grimaud, C., Bantignies, F., Pal-Bhadra, M., Ghana, P., Bhadra, U., and Cavalli, G. (2006). RNAi components are required for nuclear clustering of Polycomb group response elements. *Cell* 124, 957–971.
- Grivna, S.T., Beyret, E., Wang, Z., and Lin, H. (2006a). A novel class of small RNAs in mouse spermatogenic cells. *Genes Dev.* 20, 1709–1714.
- Grivna, S.T., Pyhtila, B., and Lin, H. (2006b). MIWI associates with translational machinery and PIWI-interacting RNAs (piRNAs) in regulating spermatogenesis. *Proc. Natl. Acad. Sci. USA* 103, 13415–13420.
- Gruidl, M.E., Smith, P.A., Kuznicki, K.A., McCrone, J.S., Kirchner, J., Roussel, D.L., Strome, S., and Bennett, K.L. (1996). Multiple potential germ-line helicases are components of the germ-line-specific P granules of *Caenorhabditis elegans*. *Proc. Natl. Acad. Sci. USA* 93, 13837–13842.
- Gunawardane, L.S., Saito, K., Nishida, K.M., Miyoshi, K., Kawamura, Y., Nagami, T., Siomi, H., and Siomi, M.C. (2007). A slicer-mediated mechanism for repeat-associated siRNA 5' end formation in *Drosophila*. *Science* 315, 1587–1590.
- Hashimoto, Y., Maegawa, S., Nagai, T., Yamaha, E., Suzuki, H., Yasuda, K., and Inoue, K. (2004). Localized maternal factors are required for zebrafish germ cell formation. *Dev. Biol.* 268, 152–161.
- Kennerdell, J.R., Yamaguchi, S., and Carthew, R.W. (2002). RNAi is activated during *Drosophila* oocyte maturation in a manner dependent on aubergine and spindle-E. *Genes Dev.* 16, 1884–1889.
- Khvorova, A., Reynolds, A., and Jayasena, S.D. (2003). Functional siRNAs and miRNAs exhibit strand bias. *Cell* 115, 209–216.
- Kimmel, C.B., Ballard, W.W., Kimmel, S.R., Ullmann, B., and Schilling, T.F. (1995). Stages of embryonic development of the zebrafish. *Dev. Dyn.* 203, 253–310.
- Kotaja, N., Bhattacharyya, S.N., Jaskiewicz, L., Kimmins, S., Parvinen, M., Filipowicz, W., and Sassone-Corsi, P. (2006). The chromatoid body of male germ cells: similarity with processing bodies and presence of Dicer and microRNA pathway components. *Proc. Natl. Acad. Sci. USA* 103, 2647–2652.
- Krovel, A.V., and Olsen, L.C. (2002). Expression of a vas:EGFP transgene in primordial germ cells of the zebrafish. *Mech. Dev.* 116, 141–150.
- Kuramochi-Miyagawa, S., Kimura, T., Yomogida, K., Kuroiwa, A., Tadokoro, Y., Fujita, Y., Sato, M., Matsuda, Y., and Nakano, T. (2001). Two mouse piwi-related genes: miwi and mili. *Mech. Dev.* 108, 121–133.
- Kuramochi-Miyagawa, S., Kimura, T., Ijiri, T.W., Isobe, T., Asada, N., Fujita, Y., Ikawa, M., Iwai, N., Okabe, M., Deng, W., et al. (2004). Mili, a mammalian member of piwi family gene, is essential for spermatogenesis. *Development* 131, 839–849.
- Lau, N.C., Seto, A.G., Kim, J., Kuramochi-Miyagawa, S., Nakano, T., Bartel, D.P., and Kingston, R.E. (2006). Characterization of the piRNA complex from rat testes. *Science* 313, 363–367.
- Lingel, A., and Sattler, M. (2005). Novel modes of protein-RNA recognition in the RNAi pathway. *Curr. Opin. Struct. Biol.* 15, 107–115.
- Liu, J., Carmell, M.A., Rivas, F.V., Marsden, C.G., Thomson, J.M., Song, J.J., Hammond, S.M., Joshua-Tor, L., and Hannon, G.J. (2004). Argonaute2 is the catalytic engine of mammalian RNAi. *Science* 305, 1437–1441.
- Meister, G., Landthaler, M., Patkaniowska, A., Dorsett, Y., Teng, G., and Tuschl, T. (2004). Human Argonaute2 mediates RNA cleavage targeted by miRNAs and siRNAs. *Mol. Cell* 15, 185–197.
- Pal-Bhadra, M., Bhadra, U., and Birchler, J.A. (2002). RNAi related mechanisms affect both transcriptional and posttranscriptional transgene silencing in *Drosophila*. *Mol. Cell* 9, 315–327.
- Parker, J.S., and Barford, D. (2006). Argonaute: a scaffold for the function of short regulatory RNAs. *Trends Biochem. Sci.* 31, 622–630.
- Rongo, C., Brohier, H.T., Moore, L., Van Doren, M., Forbes, A., and Lehmann, R. (1997). Germ plasm assembly and germ cell migration in *Drosophila*. *Cold Spring Harb. Symp. Quant. Biol.* 62, 1–11.
- Ruby, J.G., Jan, C., Player, C., Axtell, M.J., Lee, W., Nusbaum, C., Ge, H., and Bartel, D.P. (2006). Large-scale sequencing reveals 21U-RNAs and additional microRNAs and endogenous siRNAs in *C. elegans*. *Cell* 127, 1193–1207.
- Saito, K., Nishida, K.M., Mori, T., Kawamura, Y., Miyoshi, K., Nagami, T., Siomi, H., and Siomi, M.C. (2006). Specific association of Piwi with rasiRNAs derived from retrotransposon and heterochromatic regions in the *Drosophila* genome. *Genes Dev.* 20, 2214–2222.
- Schwarz, D.S., Hutvagner, G., Du, T., Xu, Z., Aronin, N., and Zamore, P.D. (2003). Asymmetry in the assembly of the RNAi enzyme complex. *Cell* 115, 199–208.
- Selman, K., Wallace, R.A., Sarka, A., and Qi, X. (1993). Stages of oocyte development in the zebrafish *Brachydanio rerio*. *J. Morphol.* 152, 203–224.
- Stajich, J.E., Block, D., Boulez, K., Brenner, S.E., Chervitz, S.A., Dagdigan, C., Fuellen, G., Gilbert, J.G., Korf, I., Lapp, H., et al. (2002). The Bioperl toolkit: Perl modules for the life sciences. *Genome Res.* 12, 1611–1618.
- Tan, C.H., Lee, T.C., Weeraratne, S.D., Korzh, V., Lim, T.M., and Gong, Z. (2002). Ziwi, the zebrafish homologue of the *Drosophila* piwi: co-localization with vasa at the embryonic genital ridge and

gonad-specific expression in the adults. *Mech. Dev.* 119 (Suppl 1), S221–S224.

Vagin, V.V., Sigova, A., Li, C., Seitz, H., Gvozdev, V., and Zamore, P.D. (2006). A distinct small RNA pathway silences selfish genetic elements in the germline. *Science* 313, 320–324.

Watanabe, T., Takeda, A., Tsukiyama, T., Mise, K., Okuno, T., Sasaki, H., Minami, N., and Imai, H. (2006). Identification and characterization of two novel classes of small RNAs in the mouse germline: retrotransposon-derived siRNAs in oocytes and germline small RNAs in testes. *Genes Dev.* 20, 1732–1743.

Weidinger, G., Stebler, J., Slanchev, K., Dumstrei, K., Wise, C., Lovell-Badge, R., Thisse, C., Thisse, B., and Raz, E. (2003). dead end, a novel vertebrate germ plasm component, is required for zebrafish primordial germ cell migration and survival. *Curr. Biol.* 13, 1429–1434.

Westerfield, M. (1993). *The Zebrafish Book* (Eugene, OR: University of Oregon Press).

Wienholds, E., van Eeden, F., Kusters, M., Mudde, J., Plasterk, R.H., and Cuppen, E. (2003). Efficient target-selected mutagenesis in zebrafish. *Genome Res.* 13, 2700–2707.

Yoon, C., Kawakami, K., and Hopkins, N. (1997). Zebrafish vasa homologue RNA is localized to the cleavage planes of 2- and 4-cell-stage embryos and is expressed in the primordial germ cells. *Development* 124, 3157–3165.

Yu, B., Yang, Z., Li, J., Minakhina, S., Yang, M., Padgett, R.W., Steward, R., and Chen, X. (2005). Methylation as a crucial step in plant microRNA biogenesis. *Science* 307, 932–935.

Zamore, P.D., and Haley, B. (2005). Ribo-gnome: the big world of small RNAs. *Science* 309, 1519–1524.

Zhang, Z., Schwartz, S., Wagner, L., and Miller, W. (2000). A greedy algorithm for aligning DNA sequences. *J. Comput. Biol.* 7, 203–214.